ACS OMEGA

Open Access

http://pubs.acs.org/journal/acsodf

Article

Natural-Based Microparticles as Sole Stabilizers of High Internal Phase Pickering Emulsions

Marie Cafiero,* Marie-Noëlle Maillard, Sabrina Maniguet, Valérie de La Poterie, and Delphine Huc-Mathis

Cite This: *ACS Omega* 2025, 10, 4534−4547

Read Online

ACCESS | Metrics & More | Article Recommendations

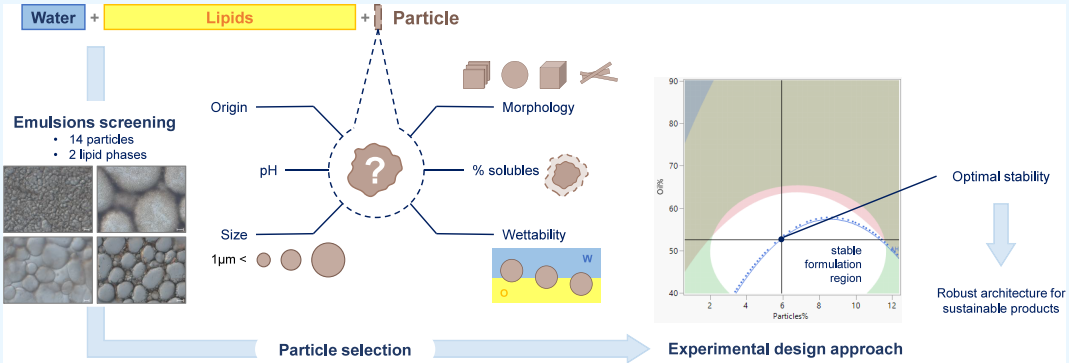

ABSTRACT: Designing a water-reduced emulsion is a technical approach to creating more sustainable cosmetic products and reducing the strain on global water resources. This study explores the structuration of highly concentrated O/W emulsions solely stabilized by particles, also known as "high internal phase Pickering emulsions" (HIPPEs). It focuses especially on particles from natural origins with a micrometric scale instead of the highly modified nanometric ones commonly used (which may raise health issues). Highly concentrated O/W emulsions were formulated with different lipid phases (regarding the chemical nature and polarity) of up to 80%. A comprehensive array of particle natural sources (plant, mineral, etc.), micrometric sizes (from 3 to 45 μm), and geometries were screened. Parameters such as droplet size distribution, microstructure, relative stability (backscatter level changes), and pH were systematically monitored over 2 weeks. An experimental design approach was carried out on three particles to determine their stability domains in various formulation combinations, dissecting complex parameter interactions that pilot emulsion characteristics. Micrometric particles demonstrated excellent efficacy in structuring HIPPEs. A wide spectrum of systems can be engineered, exhibiting a wide range of microstructures (droplets ranging from micrometers to several millimeters), stabilities, and intrinsic properties (with pH values extending from approximately 6 to 10). Emulsions displaying resistance to coalescence in W/O systems were also successfully formulated by using hydrophobic natural particles. Waterless emulsions (less than 20% (w/w) water) stabilized exclusively with naturally derived microparticles represent promising architectures for designing future clean-label cosmetic prototypes. By meticulously selecting particle parameters, including their chemical composition, size, or origin, we can tailor the architecture of HIPPEs to obtain the targeted characteristics and functionalities. Beyond particle constituents, other ingredients influence the structural arrangement such as the lipid phase chemistry.

1. INTRODUCTION

As consumers increasingly demand "clean label" alternatives for cosmetic products, the cosmetic industry is exploring new avenues to develop more sustainable formulations. Emulsions have become the preferred form in this field due to their textural properties and bicompartmental structure, allowing the solubilization of both hydrophilic and lipophilic active compounds.[1] Cosmetic products are predominantly oil-in-water (O/W) emulsions in which oil droplets are dispersed in a continuous water phase. Water serves as an inexpensive filler and a vehicle for hydrophilic active ingredients, comprising up to 85% of the composition in standard creams.[2,3]

However, the extensive use of water in cosmetic formulations is becoming controversial due to current hydric

Received: September 6, 2024
Revised: January 15, 2025
Accepted: January 16, 2025
Published: January 30, 2025

https://doi.org/10.1021/acsomega.4c08147
ACS Omega 2025, 10, 4534−4547

Table 1. Raw Material Specifications of the Studied Particles Explored in the Formulation of Emulsions

particle type	code	trade name	supplier	NI	NOI	INCI name
microcrystalline cellulose	s-MC	VIVAPUR CS 4 FM	J. Rettenmaier & Söhne, Germany	0	1	microcrystalline cellulose
microcrystalline cellulose	l-MC	VIVAPUR CS 130 FM	J. Rettenmaier & Söhne, Germany	0	1	microcrystalline cellulose
native rice starch	RS	REISITA NATURAL	AGRANA Stärke, Austria	1	1	*Oryza sativa* starch
(heat-treated) native maize starch	MS	MAISITA 9040	AGRANA Stärke, Austria	1	1	maize/*Zea mays* starch
micronized apple pomace	AP	VITACEL CS 5 APPLE	J. Rettenmaier & Söhne, Germany	1	1	Pyrus malus fiber
micronized orange pomace	OP	VITACEL CS 7 ORANGE	J. Rettenmaier & Söhne, Germany	1	1	*Citrus aurantium* dulcis fruit powder
micronized rice wax	RW	KAHLPOWDER 2811P7	Kahl, Allemagne	1	1	*Oryza sativa* Cera
diatomaceous earth	DE	IMERCARE 03D	Imerys Minerales Arica, Chile	1	1	diatomaceous earth
silica	Sil	GODD BALL G-6C	Suzuki Yushi Industrial, Japan	0	1	silica
mica	Mic	SERICITE M	K.S. PEARL, Korea	1	1	mica
zinc oxides	ZnO	ZINC OXIDE GOLD SEAL B	EverZinc, Nederland	0	1	zinc oxides
kaolin clay	KC	IMERCARE 04K	Imerys Minerals, France	1	1	kaolin
smectite clay	SC	VEEGUM HV	Vanderbilt Minerals, United States	0	1	magnesium aluminum silicate
bentonite clay	BC	KUNIPIA G	Kunimine Industries, Japan	1	1	bentonite

stress. To reduce the water footprint of cosmetics, two main targets are identified: visible water in the final product and virtual water used during the production stages.[4] Various "waterless" solutions are being explored to address these challenges, including the emergence of dry or anhydrous products, which are valued for their environmentally friendly image.[3,5] Despite this, these alternatives face consumer acceptance issues, often due to their less suitable sensory properties and lower biological efficacy compared to conventional products. Therefore, this study aims to formulate eco-friendly waterless emulsions that retain the benefits of traditional emulsions while drastically reducing water content, albeit with significant structural challenges.

Low-water-content emulsions can be currently created using two main strategies. The first involves reversing the emulsion type to water-in-oil (W/O), commonly used in makeup but less so in skincare due to the lack of freshness upon application.[6] The second strategy involves formulating high internal phase emulsions (HIPEs), characterized by an internal phase volume ratio above 0.74, leading to visco-elastic solid-like behavior.[7,8] HIPEs traditionally use large amounts of surfactants, which are controversial due to potential irritancy and environmental harm.[9,10] Alternative interfacial materials such as polymers and solid particles have been explored, though they also pose challenges.[11] Polymers, for example, can range from highly synthetic materials (e.g., grafted acrylic polymers[12]) to potentially allergenic substances such as proteins.[13,14]

A third strategy would be to anchor solid particles at the interface, and form well-known Pickering emulsions, for preventing coalescence and enhancing stability.[15] The formation of high internal phase pickering emulsions (HIPPEs) combines the advantages of HIPEs and Pickering emulsions, requiring minimal particle quantities for stabilization.[16] This "HIPPE" combination appeared in the 2000s[17] and has been increasingly used since the 2010s. Despite advancements in particle composition toward more biosourced materials, significant barriers remain: the need for extensive chemical modification of natural materials, the potential allergenicity risks in topical applications (for instance with proteins[13,14]), and the prevalent use of nanoscale particles[18] with associated health and environmental concerns.[19]

Therefore, HIPPEs can meet clean label expectations only if they are formulated with natural-based, minimally processed micrometric particles. Current literature on microparticles in HIPPEs is limited, focusing on specific components like starch crystals or modified diatomite.[20,21] This study investigates novel HIPPE designs using relatively unmodified natural-based microparticles. First, it assesses structural possibilities with a qualitative approach using a diverse panel of fourteen micrometric solid particles (selected on the basis of their size above 1 μm and a high natural origin index). Second, it targets a detailed understanding of stabilization mechanisms for waterless HIPPEs through an experimental design approach.

2. MATERIALS AND METHODS

2.1. Raw Materials. The 14 particles selected for the screening are listed in Table 1. Their natural index (NI) or natural origin index (NOI) is given as defined by standard ISO 16128.[22] Two model cosmetic lipid phases were used: a nonpolar branched C15-C19 alkane (Emogreen L15 from SEPPIC, France) and a polar medium chain triglyceride ester composed of saturated caprylic (C8) and capric (C10) fatty acids (Miglyol 812 N from IOI Oleochemicals, Germany). A more complex skeleton vegetable oil (meadowfoam seed oil) was explored as the lipid phase in the second part of this study (FANCOR MEADOWFOAM SEED OIL from Elementis, UK), dealing with the understanding of stabilization mechanisms of waterless HIPPE. The aqueous phase kept the same composition throughout the whole study: deionized water purified using ELGA PURELAB Chorus (Veolia Environment, France) and potassium sorbate (RonaCare Potassium Sorbate from Merck, Germany) added at 2.6 g L^{-1} for preservative purpose.

2.2. Emulsion Preparation. The emulsion preparation is adapted from the method proposed by Huc-Mathis et al.[23] Emulsification time and speed were adjusted to the selected particles; they are detailed in Table 2 as well as the percentage of particles used in the emulsion. The rest of the mixture was divided into 80% (w/w) of the lipid phase (alkane or triglyceride) and 20% (w/w) of the aqueous phase. The

https://doi.org/10.1021/acsomega.4c08147
ACS Omega 2025, 10, 4534−4547

Table 2. Emulsions Compositions and Specific Emulsification Processes

particle code	% (w/w) of particle in emulsion	lipid phase	emulsion code	particle dispersion	emulsification process
s-MC	3%	alkane	s-MC/A		3,000 rpm (5min)
					+ 6,000 rpm (1min)
					+ 8,000 rpm (1min)
					+ 10,000 rpm (3min)
				x	+ 12,000 rpm (2min)
		triglyceride	s-MC/T		3,000 rpm (5min)
					+ 10,000 rpm (5min)
					+ 12,000 rpm (2min)
l-MC	3%	alkane	l-MC/A		4,000 rpm (1min)
					+ 6,000 rpm (1min)
					+ 10,000 rpm (3min)
				x	+ 12,000 rpm (2min)
		triglyceride	l-MC/T		10,000 rpm (3min)
					+ 12,000 rpm (2min)
RS	5%	alkane	RS/A		4,000 rpm (2min)
					+ 10,000 rpm (3min)
					+ 12,000 rpm (2min)
		triglyceride	RS/T	x	3,000 rpm (2min)
					+ 10,000 rpm (3min)
					+ 12,000 rpm (2min)
MS	3%	alkane	MS/A		4,000 rpm (2min)
					+ 10,000 rpm (3min)
					+ 12,000 rpm (2min)
		triglyceride	MS/T	x	3,000 rpm (2min)
					+ 10,000 rpm (3min)
					+ 12,000 rpm (2min)
AP	1%	alkane	AP/A		4,000 rpm (2min)
					+ 10,000 rpm (3min)
					+ 12,000 rpm (2min)
		triglyceride	AP/T	x	3,000 rpm (2min)
					+ 10,000 rpm (3min)
					+ 12,000 rpm (2min)
OP	1%	alkane	OP/A		4,000 rpm (2min)
				x	+ 10,000 rpm (3min)
					+ 12,000 rpm (2min)
		triglyceride	OP/T		3,000 rpm (2min)
					+ 10,000 rpm (3min)
					+ 12,000 rpm (2min)
RW	5%	alkane	RW/A		4,000 rpm (2min)
					+ 10,000 rpm (3min)
				x	+ 12,000 rpm (2min)
		triglyceride	RW/T		10,000 rpm (3min)
					+ 12,000 rpm (2min)
DE	2%	alkane	DE/A		4,000 rpm (2min)
					+ 10,000 rpm (3min)
					+ 12,000 rpm (2min)
		triglyceride	DE/T	x	3,000 rpm (30s)
					+ 10,000 rpm (3min)
					+ 12,000 rpm (2min)
Sil	5%	alkane	Sil/A		4,000 rpm (2min)
					+ 10,000 rpm (3min)
					+ 12,000 rpm (2min)
		triglyceride	Sil/T	x	3,000 rpm (2min)
					+ 10,000 rpm (3min)
					+ 12,000 rpm (2min)
Mic	2%	alkane	Mic/A		4,000 rpm (2min)
					+ 10,000 rpm (3min)
					+ 12,000 rpm (2min)
		triglyceride	Mic/T	x	3,000 rpm (3min)
					+ 8,000 rpm (2min)
ZnO	5%	alkane	ZnO/A		10,000 rpm (3min)
					+ 12,000 rpm (2min)
		triglyceride	ZnO/T	x	3,000 rpm (1min)
					+ 10,000 rpm (3min)
					+ 12,000 rpm (2min)
KC	1%	alkane	KC/A		4,000 rpm (2min)
				x	+ 10,000 rpm (3min)
					+ 12,000 rpm (2min)

https://doi.org/10.1021/acsomega.4c08147
ACS Omega 2025, 10, 4534−4547

Table 2. continued

particle code	% (w/w) of particle in emulsion	lipid phase	emulsion code	particle dispersion	emulsification process
		triglyceride	KC/T		3,000 rpm (1min)
					+ 5,000 rpm (1min)
					+ 7,000 rpm (1min)
					+ 10,000 rpm (1min)
SC	1%	alkane	SC/A		4,000 rpm (2min)
				x	+ 10,000 rpm (3min)
					+ 12,000 rpm (2min)
		triglyceride	SC/T		Progressive lipid introduction
					(3,000 rpm for 10min)
BC	1%	alkane	BC/A		4,000 rpm (2min)
					+ 10,000 rpm (3min)
					+ 12,000 rpm (2 min)
				x	
		triglyceride	BC/T		Progressive lipid introduction
					(3,000 rpm for 10min)

emulsion preparation is a two-step process. First, the particle powder is dispersed in one of the phases (most often in the lipid phase) using a single air-gap rotor-stator Ultra-Turrax (T 25, IKA Labortechnik, Germany) for 3 min at 10,000 rpm. After this priming step, the other phase is added (all at once, unless specified) to the previous mixture, and emulsification is carried out using the same mixing device (Table 2). The emulsions were stored in closed glass vials at 30 °C for a 14 day period.

2.3. Particle Characterization Methods. *2.3.1. Particle Size Distribution.* Particle size distribution was measured for each particle by using a Mastersizer 3000 analyzer (Malvern Instruments, UK). Measurements were carried out in dry (Aero 3000) and wet (Hydro 3000) cells to assess the particle size in both its native powder and hydrated states. A 2% (w/w) particle dispersion was prepared in distilled water (3 min at 10000 rpm) to be measured in wet mode. The measurements were carried out at room temperature. Particle size distribution was expressed as volume of particles (%) = f(size (μm)) and the volume median diameter $d50$ was selected as preferential index (all the selected particles displayed a monomodal distribution mode). A swelling index (Sw%) was calculated with eq 1.

$$\mathrm{Sw\%} = 100 \times \frac{d50_{\mathrm{wet}} - d50_{\mathrm{dry}}}{d50_{\mathrm{dry}}} \quad (1)$$

with $d50_{\mathrm{dry}}$ and $d50_{\mathrm{wet}}$ respectively standing for the dry and wet median diameters.

2.3.2. pH of the Dispersions. Particle dispersions were prepared in distilled water (preserved with potassium sorbate at 2.6 g L^{-1}). The percentage of particles in the aqueous phase, agitation time, and speed were the same as those applied in the previous Emulsion Preparation section (see Table 2). The pH of the particle dispersion (pH_{aq}) was measured at room temperature with a standardized pH meter (Seven Easy, Mettler Toledo, Switzerland).

2.3.3. Dry Matter and Soluble Content. The measurement method was adapted from Hollestelle et al.[24] The powder sample was dried for 7 h at 105 °C in an oven (EM10, CHOPIN Technologies, France) and cooled down for 1 h at room temperature in a desiccator. Its dry matter content dm% (w/w) is given by the formula:

$$\mathrm{dm\%} = 100 \times \frac{m_f}{m_i} \quad (2)$$

with m_i and m_f being the sample masses before and after drying, respectively.

A particle dispersion representative of the particle/water ratio of the emulsion was prepared and centrifuged at 14000 rcf for 15 min at 20 °C. The supernatant was collected, dried for 7 h at 105 °C, cooled for 1 h at room temperature, and weighed. The particle soluble content (sol%) was calculated according to the following equation:

$$\mathrm{sol\%} = 100 \times \mathrm{dm\%}_{\mathrm{supernatant}} \times \frac{m_{\mathrm{supernatant}}}{m_{\mathrm{particles}}} \quad (3)$$

with $\mathrm{dm\%}_{\mathrm{supernatant}}$ being the dry matter content of the supernatant (according to eq 2), $m_{\mathrm{supernatant}}$ the mass of supernatant sampled, and $m_{\mathrm{particles}}$ the mass of particles dispersed in the centrifuged suspension. The insoluble content (insol%) is given by

$$\mathrm{insol\%} = 100 - \mathrm{sol\%} \quad (4)$$

2.3.4. Three-Phase Contact Angle (θ). The three-phase contact angle (θ) measurement methodology was adapted from Zhang et al.[25] The θ was determined using a Drop Shape Analyzer (DSA 100, KRÜSS, Germany). The sample powders were compressed into tablets with a pelletizer (5 Mbar applied on 1 g of powder). After being immersed for 15 min in a triglyceride oil bath, a high-precision syringe was used to apply a drop of 0.8 μL of pure water onto the surface of each tablet. The images were captured by the high-speed camera (16 frames/second). The θ was performed in triplicate.

2.4. Emulsion Characterization Methods. *2.4.1. Backscattering Profile.* The backscattering and transmission profiles of samples were recorded using a Turbiscan LAB (Formulaction, France). The samples were scanned at different times: just after emulsification (t0), after 7 days (t7), and 14 days (t14) of storage. Several indexes were built based on the backscattering data. The microstructural index (bs_0) corresponds to the average backscattering level measured at the curve plateau right after emulsification (at t0). This quantitative data reflects both the element size and concentration in the emulsion. It was therefore considered as a microstructural index. A second index was calculated,

https://doi.org/10.1021/acsomega.4c08147
ACS Omega 2025, 10, 4534−4547

Table 3. Coordinates of Central Composite Design for Emulsions Across Three Factors (Composition and Process) at Three Levels

sample code	CCD			oil% (wt %)	particle% (% wt)	process (time at 10,000 rpm after the priming step)		
						s-MC	OP	BC
E1	−	−	−	50	3	2 min 35 s	2 min 50 s	1 min 25 s
E2	−	+	+	50	10	4 min 35 s	4 min 50 s	3 min 25 s
E3	0	+α	0	65	12.4	3 min 35 s	3 min 50 s	2 min 25 s
E4	+	−	+	80	3	4 min 35 s	4 min 50 s	3 min 25 s
E5	+	−	−	80	3	2 min 35 s	2 min 50 s	1 min 25 s
E6	0	0	0	65	6.5	3 min 35 s	3 min 50 s	2 min 25 s
E7	0	0	0	65	6.5	3 min 35 s	3 min 50 s	2 min 25 s
E8	0	0	−α	65	6.5	1 min 55 s	2 min 05 s	0 min 40 s
E9	0	−α	0	65	0.6	3 min 35 s	3 min 50 s	2 min 25 s
E10	−	+	−	50	10	2 min 35 s	2 min 50 s	1 min 25 s
E11	0	0	+α	65	6.5	5 min 20 s	5 min 30 s	4 min 05 s
E12	+	+	−	80	10	2 min 35 s	2 min 50 s	1 min 25 s
E13	−α	0	0	39.8	6.5	3 min 35 s	3 min 50 s	2 min 25 s
E14	+	+	+	80	10	4 min 35 s	4 min 50 s	3 min 25 s
E15	−	−	+	50	3	4 min 35 s	4 min 50 s	3 min 25 s
E16	+α	0	0	90.2	6.5	3 min 35 s	3 min 50 s	2 min 25 s

accounting for the main instability index (Δbs). Δbs is the percentage of the evolution of the backscattering level at the curve plateau between emulsification and after 14 days of storage. It is given by the following formula:

$$\Delta bs = \frac{(bs_0 - bs_{14})}{bs_0} \quad (5)$$

When the Δbs reaches high positive values, it indicates a potential colloidal instability (coalescence): droplets are larger or/and fewer in number over time. Reciprocally, when reaching negative values, it could refer to gravitational instabilities. The index used to indicate gravitational instabilities is Δh and is calculated according to

$$\Delta h = \frac{(h_0 - h_{14})}{h_0} \quad (6)$$

with h_x being the height of the emulsion in the sample after x days of storage. When creaming or sedimentation occurs, droplets migrate toward the top or bottom of the sample, conducive to a smaller height of the total emulsion and a denser layer of droplets. A creaming or sedimentation event is defined by the combination of a negative Δbs and a high Δh. The perfectly stable state is only reached when Δbs = 0 and Δh = 0 (no change in microstructure over time).

2.4.2. Optical Microscopy and Droplet Size Distribution. Emulsions' microstructure (droplet shape and arrangement) was observed at 10×, 20×, and 40× magnifications using a transmitted light microscope (Axio Imager.A1, Carl Zeiss Microscopy, Germany). When possible, the average droplet diameter in number (μ-size) and the polydispersity index (PDI) were estimated by image analysis with ZEN 2 software (Carl Zeiss Microscopy, Germany). The emulsions were observed at t0, t7, and t14.

2.4.3. Confocal Laser Scanning Microscopy. A part of the emulsions was studied under a reversed Confocal Laser Scanning Microscope (TCS SP8, Leica, Germany). HIPPE samples were stained with a drop of the fluorescent probe Nile Red 552/636 (ThermoFisher Scientific, USA) to dye the lipid phase. The obtained mixture is then placed on a coverslide and observed with 10x magnification.

2.4.4. pH of the Emulsions. The pH of the emulsions ($pH_{em.}$) was measured at room temperature with a pH meter (Seven Easy, Mettler Toledo, Switzerland) equipped with a dedicated electrode (InLab Viscous, Mettler Toledo, Switzerland).

2.5. Statistical Analysis and Mapping. *2.5.1. Overall Statistical Analyses.* In this screening approach, most of the measurements described previously were carried out in triplicate. When this was the case, as indicated in the previous sections, the significance of observed differences was verified by an ANOVA test with a 95% trust interval using XLSTAT (Addinsoft, USA). Additional statistical analyses such as PCA (Principal Component Analysis) or k-mean classifications were also performed with the same software.

2.5.2. Experimental Design. Among the 14 screened particles, three were selected as representative models for further investigation through experimental design. Experiments were carried out in order to predict the formulation conditions for stable emulsions. To increase the realism and better match the composition of a real cosmetic system, the oil phase used in this experimental section was meadowfoam seed oil. This vegetable oil is one of the most common vegetable oils used in skincare products.[26,27] A central composite experimental design (CCD) was carried out on three particles (s-MC, OP, and BC). The trials were planned to follow a three-factor central composite design (on 3 levels, i.e., 16 samples including a repeated central point). The independent factors for stability investigation were the oil content (oil%), from 50 to 80 wt %, the particle content (particle%), from 3 to 10 wt %, and the number of rotations undergone by the mixture during emulsification (process) from 23,000 to 57,000. During emulsification, a first dispersion step was carried out for all emulsions at 3000 rpm and then emulsification at 5000 rpm (time adjusted per particle, with 30 s at 3000 and 5000 rpm for s-MC, 15 s at 3000 and 5000 rpm for OP, and 2 min at 3000 and 5000 rpm for BC). The α axial value was 1.682 to ensure design rotability. The coordinates of the experimental designs are available in Table 3.

The samples were stored over a 14 day period, and backscattered light data (bs, Δbs, and Δh) were collected as Y. There is a postulated quadratic model per measured variable Y.

https://doi.org/10.1021/acsomega.4c08147
ACS Omega 2025, 10, 4534−4547

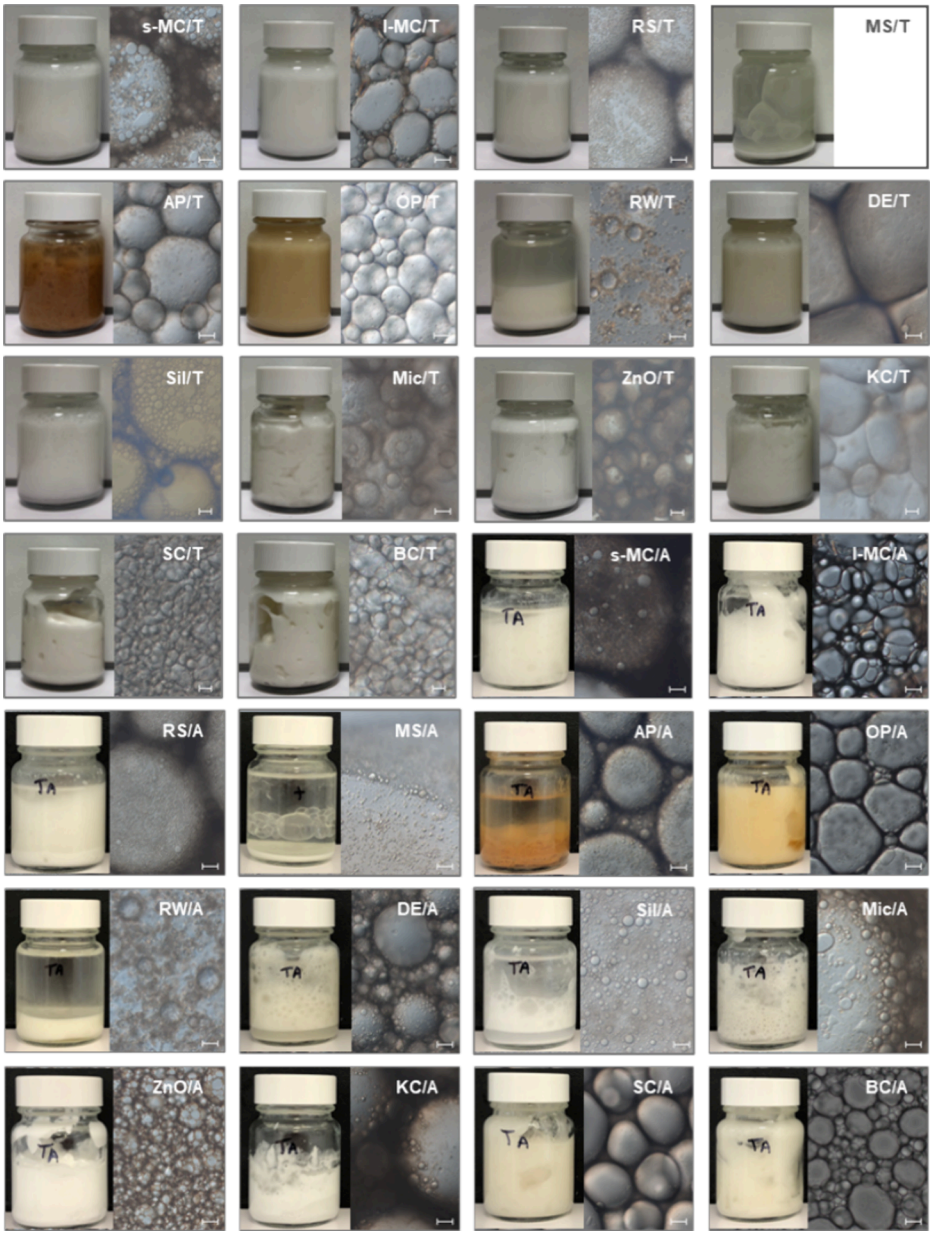

Figure 1. Samples images of the prepared in triglyceride (T) or alkane (A) emulsions and their corresponding light microscopy images (the white scale bar corresponds to 50 μm).

Each model was separately adjusted by considering effects that allow a significant model variance analysis (with p-value lower than 0.05). Statistical analyses were performed with XLSTAT software (Addinsoft, USA) and JMP Pro 16 software (SAS, Cary, North Carolina, USA).

3. RESULTS & DISCUSSION

3.1. Screening Approach. *3.1.1. Diversity of the Studied Systems.* A first exploratory screening step was carried out on the matrices formulated from the particles panel. Macro and micrometric structures of the obtained systems are illustrated in Figure 1. The microscopy images clearly show emulsion templates with identifiable droplets. These observations confirm the initial postulate that it is possible to structure HIPEs using solely natural-based microparticles, including unrefined ones. In most cases, when particles are visible under the microscope, they are mainly located at the droplet interface and partly in the continuous phase. As previously mentioned, even if the Pickering effect is strongly presumed in most of these systems, emulsion stabilization could be achieved by diverse mechanisms. They usually involve the continuous phase and/or the interfacial film.

For instance, structuring a three-dimensional network (of particles or soluble compounds) in the continuous phase immobilizes droplets and helps to stabilize dispersed systems by entrapping them.[28] From an interfacial perspective, such systems could be considered Pickering emulsions, while a more general approach might classify them as emulsion gels. Regarding the interfacial area, insoluble (solid particles) and soluble (amphiphilic or thickening compounds) fractions could interact to impact the overall stability as shown by Hollestelle et al.[24] who proved the existence of hybrid interfaces in Pickering-like emulsions stabilized by unrefined powders. To better understand the stabilization mechanisms

https://doi.org/10.1021/acsomega.4c08147
ACS Omega 2025, 10, 4534−4547

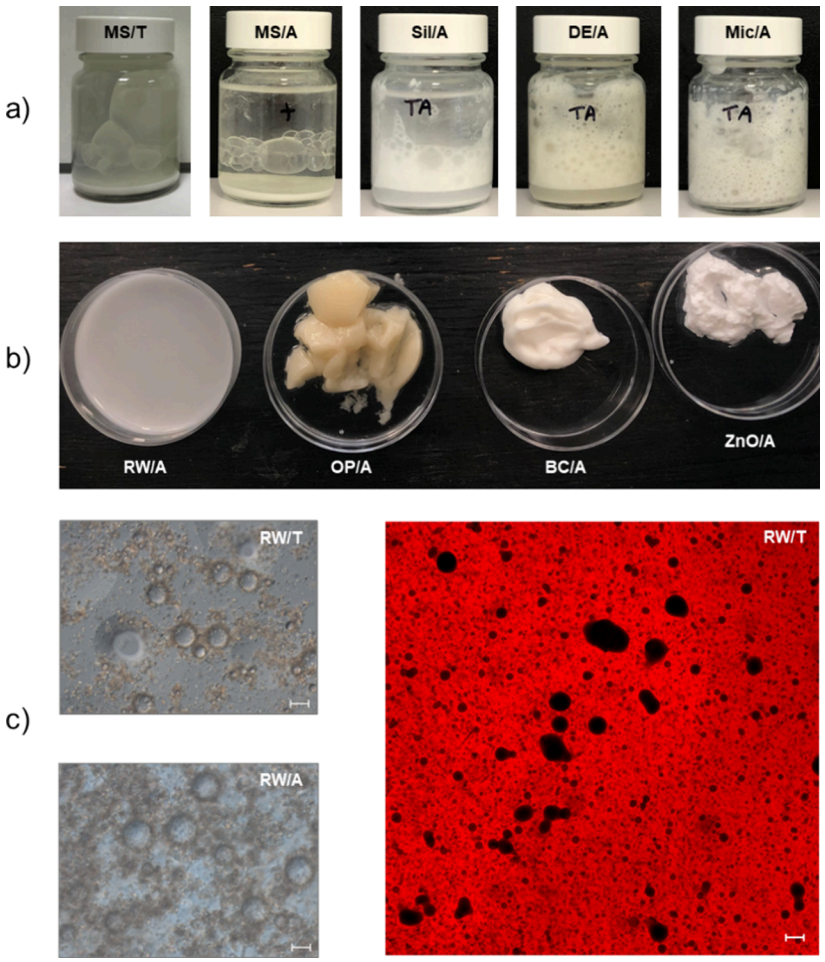

Figure 2. (a) Samples images of the prepared in triglyceride (T) or alkane (A) emulsions; (b) sample image of alkane prepared emulsions; (c) light and confocal microscopy images of RW prepared with triglyceride (the white scale bare corresponding to 50 μm).

involved and to consider possible interactions, integrative approaches are thus required.

Incorporating particles into lipid-rich systems results in a wide range of structures and properties. From the macroscopic point of view, these matrices do not present the same aspect and homogeneity; some of them exhibit some particle sedimentation (MS) and/or partial phase shift (AP/A) or draining (DE/A, Sil/A) while others are visually stable (OP, SC, BC). Different colors are obtained from the classic off-white or cream tones to more unusual brown shades formulated with AP or OP. It should be noted that MS and Mic/A samples present stable oil droplets even though they were as big as being visible to the naked eye (Figure 2a). This phenomenon was already observed in literature but to the best of our knowledge, only with chemically treated nanoparticles.[29] Finally, it is noted that the obtained panel of textures is wide, from liquid (RW) to firmer (BC) and even gelled systems (OP) (Figure 2b). Several cosmetic functionalities could thus arise from such diverse properties.

Regarding the microstructure of these matrices, another discriminant factor to consider is the emulsion's internal arrangement. A reverse emulsion template was obtained with RW for both triglyceride and alkane lipid phases. This hypothesis would explain the observed liquid texture and the "sedimentation" phenomenon observed in RW samples. This was confirmed by confocal microscopy (Figure 2c). The lipid phase (colored here in red) surrounds dark spherical shapes previously identified as emulsion droplets. The lipidic composition of the micronized rice wax particle makes it mostly hydrophobic, leading to a contact angle between the two phases of emulsion more in favor of a W/O interfacial curvature rather than an O/W interface.[30] While diverging from the targeted HIPE objective, this unexpected result provides an innovative proof-of-concept for W/O emulsions stabilized solely by plant-sourced particles. The other particles lead to O/W direct emulsions (with different stability behaviors ranging from very stable to creaming and/or phase shifting). The diverse droplet organizations range from a very fine network of micrometric droplets (~25 μm for BC/T) to much larger objects (~670 μm for s-MC/A). Except for macroscopic droplets, the average droplet diameter measured under the microscope is about 180 μm, all lipid phases considered. It is surprisingly close to standard droplet sizes mentioned in literature for Pickering emulsions, usually from 10 to 100 μm.[31] Even if this order of magnitude is higher than for emulsions stabilized with common emulsifiers (surfactant, amphiphilic polymers, etc.), microparticles do not seem to drastically increase the resultant droplet diameter compared to other Pickering emulsions. Concerning the distribution of droplet size, the formulated emulsions generally exhibit a narrow droplet size distribution, characterized by an average PDI of 0.21 in both lipid phases. Emulsions OP/T and DE/T display particularly low PDI values of 0.09 and 0.07, respectively. While monodisperse distributions are commonly

https://doi.org/10.1021/acsomega.4c08147
ACS Omega 2025, 10, 4534−4547

Table 4. Properties of Particles Used in the Formulation of Low-Water Content Emulsions

code	origin	theoretical morphology	d50dry	d50 wet	Sw%	%sol	$pH_{aq.}$	θ
s-MC	plant	needle-like	4.3 μm (±0.0)	5.6 μm (±0.1)	31.9%	0.3% (±1.1)	6.83	20.4° (±0.7)
l-MC	plant	needle-like	120.0 μm (±0.2)	44.9 μm (±3.2)	−62.6%	3.1% (±0.6)	7.25	34.1° (±0.8)
RS	plant	angular	6.6 μm (±0.0)	6.5 μm (±0.1)	−1.5%	2.8% (±0.3)	6.56	32.5° (±1.8)
MS	plant	globular	12.2 μm (±0.0)	13.5 μm (±0.1)	10.7%	0.6% (±0.3)	6.19	23.2° (±1.2)
AP	plant	heterogeneous	3.5 μm (±0.0)	6.0 μm (±0.0)	68.6%	25.8% (±0.2)	6.03	71.4° (±0.6)
OP	plant	heterogeneous	3.9 μm (±0.0)	6.0 μm (±0.0)	56.6%	52.0% (±1.3)	5.98	42.3° (±1.4)
RW	plant	angular	8.7 μm (±0.1)	33.1 μm (±4.5)	278.7%	0.6% (±2.0)	6.07	76.1° (±0.8)
DE	fossil	heterogeneous	2.6 μm (±0.0)	3.2 μm (±0.0)	25.1%	0.6% (±0.6)	7.66	39.4° (±4.3)
Sil	mineral	spherical	3.1 μm (±0.0)	4.2 μm (±0.0)	34.5%	−0.1% (±0.3)	6.21	26.1° (±1.2)
Mic	mineral	platelet	6.1 μm (±0.0)	7.2 μm (±0.0)	19.0%	0.1% (±0.4)	6.89	46.4° (±4.1)
ZnO	mineral	angular	6.4 μm (±2.1)	2.8 μm (±0.2)	−56.3%	0.2% (±0.2)	8.90	83.4° (±0.3)
KC	mineral	platelet	4.0 μm (±0.0)	4.7 μm (±0.3)	19.7%	0.7% (±0.3)	6.96	71.9° (±1.9)
SC	mineral	platelet	nd	3.5 μm (±0.0)	nd	33.5% (±8.1)	9.13	71.8° (±1.7)
BC	mineral	platelet	nd	3.0 μm (±0.2)	nd	68.4% (±6.5)	9.80	41.9° (±2.4)

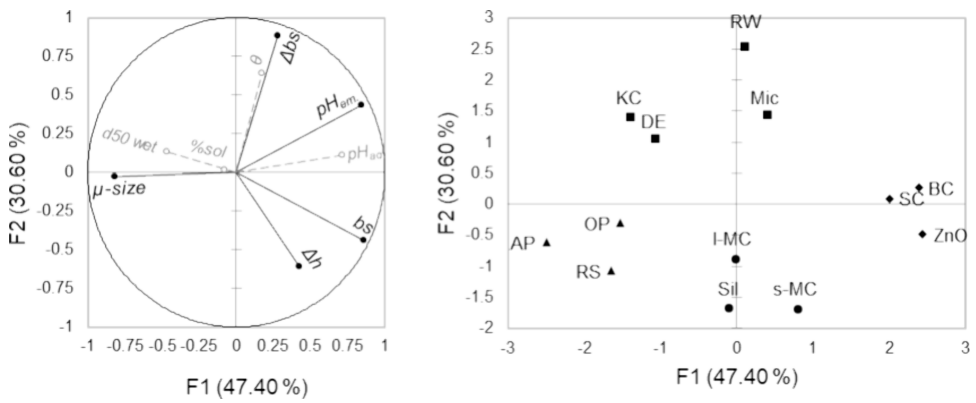

Figure 3. Correlation circle with emulsions characterization parameters as constitutive variables in black full line and particles parameters as supplementary variables in gray dotted line and PCA map of (F1; F2) for the 13 emulsions formulated with triglyceride lipid phase (with diamond solid as group 1, triangle up solid as group 2, box solid as group 3, and circle solid as group 4).

associated with arrested coalescence, a hallmark of Pickering emulsions,[30] directly attributing the observed low PDI values solely to the Pickering effect warrants careful consideration.

These emulsion templates, which we will refer to as "architectures" in the rest of this study, can be reached with very simple waterless compositions (oil + water + particles) and open a large spectrum of possibilities. To provide a deeper understanding, certain properties of the particles were characterized to provide a deeper understanding of the emulsion's behavior, several properties of the particles were characterized.

Particles were selected to purposely represent a diverse array of attributes. In that regard, the 14 studied particles displayed various natural-based origins (from plant- to mineral-based), morphologies (from isotropic to anisotropic particles), chemical compositions, and potential wettabilities in oil and water. Their only two common points are their micrometric size and the fact that they have undergone little or no modification (any modification resulting in a reduction of the NOI below 1 was excluded). The main physicochemical properties measured on the 14 studied particles are summarized in Table 4.

When dispersed in water, the particles exhibit $pH_{aq.}$ values from around 6 to 10, covering a wide range of possibilities (6 being in the skin's pH range[32]). Particle contact angles (θ) do not exceed 90°, which typically indicates an O/W emulsion structure according to the literature. However, one of the maximum values is attributed to the RW with a θ of 76°. According to the confocal microscopy images in Figure 2c, the resultant structures diverge from the expected characteristics of O/W systems. This observation calls into question the relevance of the wettability measurement method. Specifically, it casts doubt on whether compressed powder truly reflects the real conditions of the systems. With regard to particle dimension, the measured wet size (*i.e.*, when dispersed in water) is between 2 and 35 μm. This diameter is completely out of scope compared to conventional HIPPEs where Pickering particles usually measure only a few hundred nanometers, that is 20 to 350 times less. This screening approach demonstrates that "large" particles can efficiently stabilize HIPPES. However, the Pickering mechanism as defined in the literature[33,34] must be considered with caution not only in the case of micron-sized but also in complex particles. Indeed, in pure Pickering emulsions, stability is derived solely from solid particles anchored at the interface. In this study, the studied particles are not all composed only of insoluble materials, as shown by their soluble content. This is notably true for AP, SC, OP, and BC, with soluble contents ranging from 25% (w/w) to 70% (w/w). This may have minimal impact on emulsification[35] or may contribute to stability (through synergistic competitive interactions between particle fractions) while for other particles such as Sil, Mic, or s-MC, a classic Pickering effect could be reasonably postulated based on their very large insoluble fraction.

https://doi.org/10.1021/acsomega.4c08147
ACS Omega 2025, 10, 4534−4547

This preliminary overview assesses the diversity of the selected samples and provides essential insights for a better comprehension of the results related to the interfacial materials. The diversity of the panel raises the question of structures and mechanisms, going from pure Pickering to potential hybrid interfaces). To draw the first hypotheses from these various observations, the first question was to assess the particle effect and the second was to estimate the lipid effect on the resultant emulsion architectures.

3.1.2. Effects of Constitutional Factors on Emulsion Architecture. 3.1.2.1. Particle Impact. The objective of this section is to investigate the impact of the particle type on the resulting emulsions. A broad, not exhaustive, set of parameters was investigated to encompass the full diversity of our representative panel of natural-based particles. Microstructure (bs), stability (Δbs and Δh), pH_{em}, and droplet size (μ-size) are examined at first for a defined lipid type (triglyceride). The samples are mapped according to their physical properties in order to identify the main structure−function underlying relationships based on a PCA as can be seen in Figure 3.

The two axes represent 78% of the overall information. All variables are close to the correlation circle and therefore well represented. The product space is well-covered by the samples, where none was found in the center of the PCA map. As developed in the previous section, MS droplet size was too large to be estimated under an optical microscope. Due to this missing data, this particle was removed from Figure 3 mapping.

The x-axis F1 is mostly driven by the droplet size which is significantly anticorrelated to bs (correlation coefficient of −0.7, p-value < 0.05). As expected, the bigger the droplets, the smaller the backscattered light level. Consequently, the F1 axis carries most of the structural information. The F2 axis, on the other hand, rather represents the instability elements (Δbs and Δh). Unexpectedly, Δbs (the variation of backscattering signal with time) is orthogonal to the structural variables (bs and μ-size), suggesting that the droplet size has no impact on the stability of the system. This is not the case in most classical emulsions, where good physical stability is usually associated with smaller droplets. The interfacial nature of these systems could be an explanation for this. In Pickering emulsions, the droplet size is directly driven by the particle diameter.[36] So, by using micrometric particles, extra-large and stable droplets are accessible. Their irreversible adsorption (in Pickering emulsions) leads to unusually big (≫100 μm) but still stable droplets with time.

The particle properties were projected on the PCA map as additional variables. Contact angle θ is positively correlated to Δbs (correlation coefficient of 0.6, p-value < 0.05). This indicates that the higher θ, the higher Δbs, the more unstable the system. It goes against current knowledge which claims that the closer the system is to 90°, the more stable it is. In another hand, no clear correlation could be drawn from them because variables such as d50wet and %sol are not well enough represented on the F1 and F2 axes. Therefore, contact angle, particle size, and soluble vs insoluble fractions are not the sole factors driving the diversity of physical properties obtained for the formulated HIPPEs. Other parameters such as shape,[37] surface roughness,[38] size, and charge[39] or surface-active properties of the soluble compounds[24] could be as much as other leads. Further investigations could explore more specific and well-known particle properties using a more targeted selection of candidates. Alternatively, rather than studying particle properties individually, future research could investigate combinations of parameters to account for potential interactions.

Finally, among the emulsion population, four different groups can be formed by statistical analysis (k-mean classification on the F1/F2 data set). The obtained groups can be referred to as such: group 1: with high bs (dense close-packed organization), group 2: with high μ-size (large droplets), group 3: with high Δbs (coalescence instability), and group 4: with high Δh (gravitational instability) on Figure 3. According to ANOVA tests, groups 1 and 2 are significantly different on the x-axis (F1). These groups thus mostly differ from each other due to their microstructure: group 1 with a close-packed organization (mean bs = 70%), group 2 with big droplets (mean μ-size ≈ 200 μm). On the other hand, groups 3 and 4 are significantly different on the y-axis (F2), showing different stability behaviors. Group 3 is more sensitive to coalescence while group 4 is more sensitive to creaming/sedimentation. These results emphasize again the independence between the droplet size and the relative physical stability of the HIPPEs. As previously mentioned, %sol. is not explicitly represented on the F1/F2 axis, but it is noteworthy that group 3, characterized by low coalescence stability, consists solely of insoluble particles (KC, DE, RW, Mic). While coalescence-stable HIPEs can be achieved with both purely insoluble and partially soluble particles, the latter may be preferable due to fewer limitations. Soluble content may offer a primary selection criterion for identifying promising candidates.

Thanks to its diversity, this panel of architectures covers a wide scope of structures and behaviors regarding physical stability. It appears that the particle nature plays a crucial role in the architectural design. Different compositional factors should be investigated to explore other formulative possibilities in relation to the emulsions' properties. In a later section, general connections between architectures and their constituent particles are explored, building upon the initial screening approach.

3.1.2.2. Lipid Impact. As the lipidic phase represents 80% of the system, investigating its sensitivity to lipid phase composition is a pivotal step in extending such matrix into functional products. In that perspective, two cosmetic-grade lipid phases have been compared in emulsion: medium-chain triglyceride and a very nonpolar branched alkane.

The obtained populations exhibit individual differences from one particle type to another. In brief, lipids impact the resultant architecture in a particle-dependent way. The only variable that follows the same tendency among all the particles is the droplet size (μ-size) going from an average of 130 μm in diameter with triglyceride to an average value higher than 470 μm with alkane. In our studied systems, nonpolar branched alkane tends to favor the formation of bigger droplets compared to medium-chain triglyceride.

In order to focus on the lipid impact, specific variations were illustrated with the mapping shown in Figure 4a. It is built on a two-dimensional space with one axis referring to the microstructure (inner architecture of the system on the x-axis) and the other referring to its stability (evolution of the system over time on the y-axis). Each of these dimensions is represented by an index calculated from the Turbiscan LAB backscattering analyses (bs and Δbs, respectively). This map presents the two samples' populations formulated with triglyceride (black dots) or alkane (white dots) lipid phase with the composition ratio. The difference between two paired samples is represented with a gray line. Depending on the

https://doi.org/10.1021/acsomega.4c08147
ACS Omega 2025, 10, 4534−4547

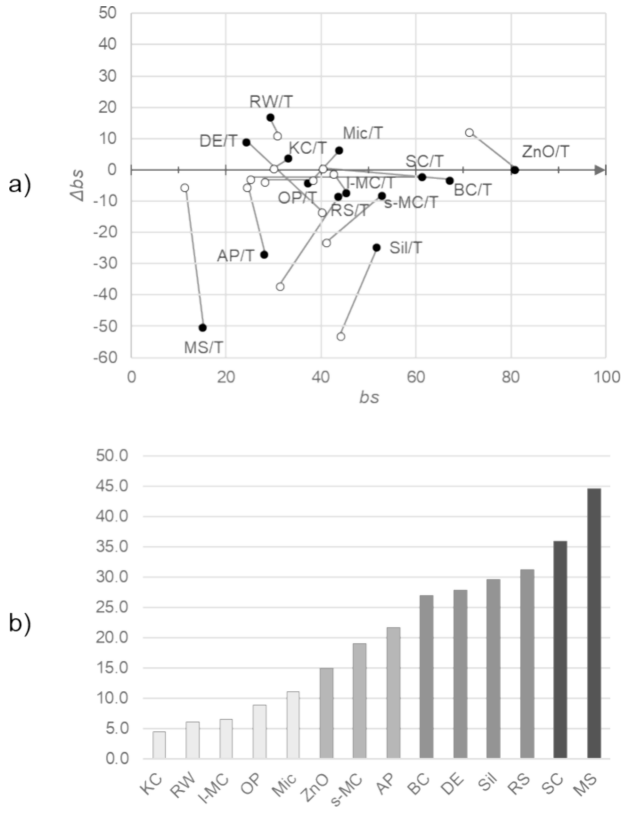

Figure 4. (a) Mapping of emulsion populations (circle solid for the triglyceride-based emulsions, circle open for the alkane-based emulsions) with the microstructure index (bs) as *x*-axis and the instability index (Δbs) as *y*-axis, each pair being connected by a gray line; (b) norms of the vectors corresponding to the translation from the position of triglyceride emulsion to its alkane equivalent in the map $f(\text{bs}) = \Delta\text{bs}$.

particle type, various behaviors emerge. Some emulsions are similar regardless of the lipid type used (KC, RW), while others show clearly different microstructures (SC, BC) and/or stabilities (MS, Sil).

This difference between the paired architectures was approached by calculating the norm of the vector connecting the triglyceride emulsion to its alkane equivalent (Figure 4a). It is possible to class these architectures with regard to their lipid sensitivity: the more the architecture evolves from one lipid phase to another, the more they are considered lipid-sensitive. Four significantly different groups can be identified through a statistical analysis (k-mean classification method on vectors' norms), all illustrating different levels of lipid sensitivity. The nonsensitive group (light gray) exhibits a norm value under 15, the slightly sensitive group (in medium gray) between 15 and 25, the sensitive group (in dark gray) between 25 and 35, and the very lipid-sensitive group (in black) a norm value above 35.

Even if solid particles lead to various properties, no exploitable correlation between architecture lipid sensitivity and the measured physical properties, of particles could be found so far. This section highlights that none of the studied particles are universally superior. When it comes to natural-based minimally processed candidates, particle selection must be made in accordance with the intended application and desired properties of the resulting systems.

Investigating the impact of particle/lipid interactions could be an interesting lever to design systems with tuned structure and stability. Beyond lipid sensitivity, several other formulation and compositional parameters merit further investigation. Exploring diverse emulsification processes, such as ultrasonication or high-pressure homogenization as well as varying shearing intensity, could expand the range of potential systems. Additionally, a more targeted panel could assess the influence of specific particle parameters, including size, charge, etc. These novel systems might require a departure from conventional approaches, necessitating the use of nonstandard markers.

3.2. Prediction of Emulsion Stability by an Approach by Experimental Design. As genericity is a challenge with such a diverse panel, a few particles were selected as representative of this wide product space for further study using an experimental design. This approach supplements the previous section by providing information about the interactions among the examined variables.

In order to mimic the composition of a cosmetic lipid phase and knowing that particles exhibit specific lipid sensitivity, the meadowfoam seed oil was selected as a complex and natural lipid model phase for the experimental design.

OP exhibits promising properties and versatility (Figures 3 and 4b). It was selected as a complex plant-based low-processed particle (with an NI of 1) and circular-based ingredient (food byproduct) for further study. In addition, this raw material was already studied in previous works[23,40] and appears to be compatible with the structuration of HIPPE, leading to a droplet size around 120 μm.[23] As its OP soluble content is high (52%), BC was selected to represent its mineral analogue, similar in size, and also with a high soluble fraction (68%). The third and last particle chosen in this study, s-MC, stands for an almost 100%-insoluble more conventional Pickering particle. Its diameter is in the same size range as OP and BC, and its cellulosic composition matches that of OP. This selection was designed to compare the impacts of particles' chemical (cellulosic/silicate) and physical (soluble/insoluble) natures without falling into a very obvious particle size effect. Moreover, as the three particles belong to different groups in the previous classifications, they are expected to behave differently under the CCD approach. For instance, in Figure 3, OP presents large droplets while BC presents a close-packed organization and s-MC a gravitational instability. They also belong to different lipid sensitivity groups (nonsensitive, sensitive, and slightly sensitive in Figure 4b). These three particles underwent identical experimental design settings to compare their stability behaviors. The input variables cover a wide range of formulations in terms of composition and process parameters. The maps for three levels of process, low (−), average (0), and high (+) are available in Figure 5. Once fitted, the predictive models for OP, BC, and s-MC had R^2 values of (0.96, 0.99, 0.69), (0.85, 0.35, 0.65), and (0.84, 0.64, 0.41) for bs, Δbs, and Δh respectively. The experimental design encompassed a broad spectrum of formulations, acknowledging that some would fail to form emulsions. Formulations that resulted in a bs of less than 50% were predetermined as nonemulsifying and are designated in red in Figure 5. Among the emulsified systems, the ones with "acceptable" stability (characterized by Δbs and Δh within −10 to 10%) appear in white in Figure 5 for easy identification. The stability domain indicates formulas predicted as stable emulsions and represents an exploration area for future product formulation. It reduces the scope for exploration to directly lead to stable and robust proofs of concept. To go even

https://doi.org/10.1021/acsomega.4c08147
ACS Omega 2025, 10, 4534−4547

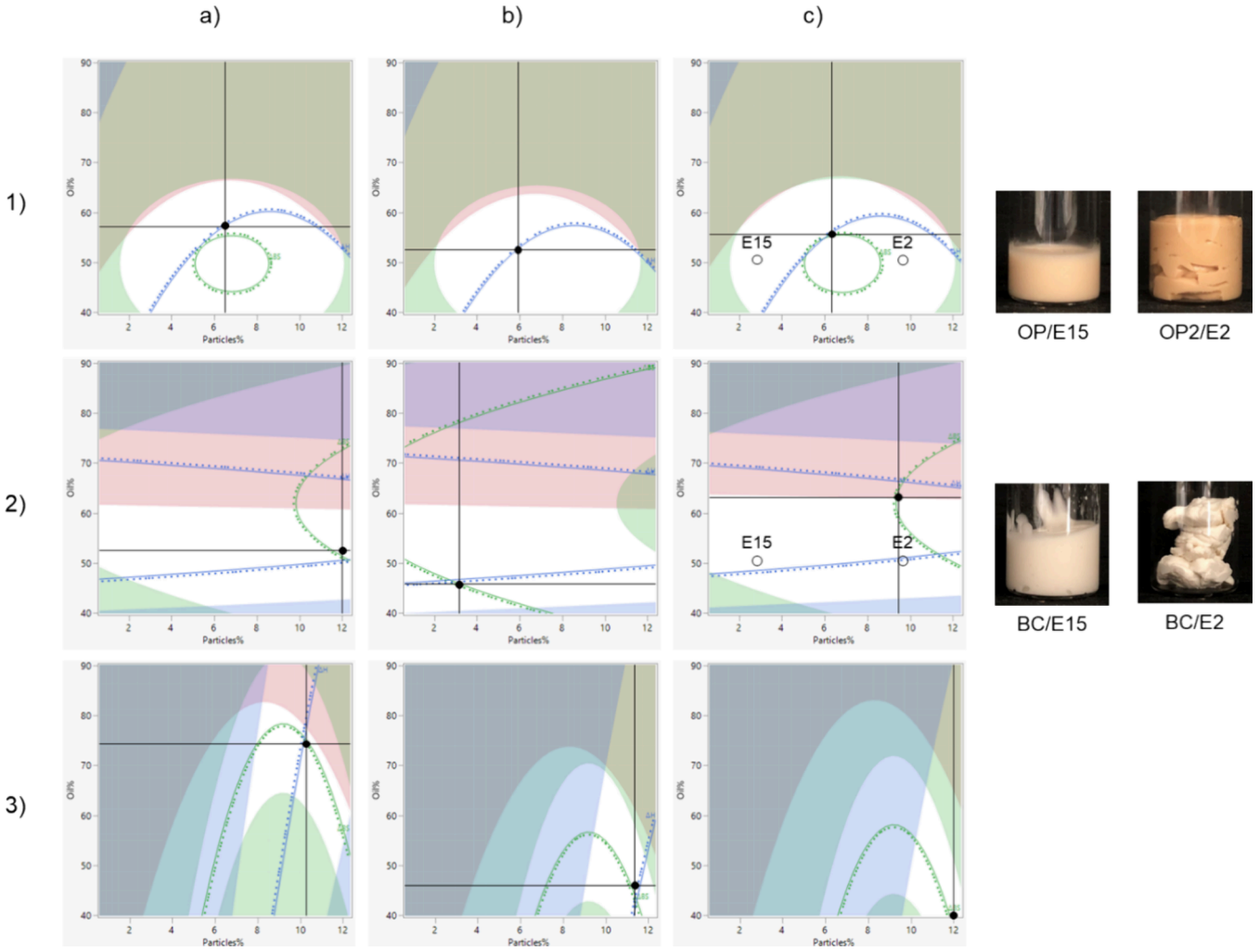

Figure 5. Iso-response profiles for the emulsions prepared with (1) OP, (2) BC, and (3) s-MC in different process conditions, (a) at low, (b) medium, and (c) high emulsification times and pictures of CDD samples predicted as stables represented by white dots on the map. The colored areas correspond to: $\Delta bs < -10\%$ or $\Delta bs > 10\%$ for the green one, $\Delta h < -10\%$ or $\Delta h > 10\%$ for the blue one, and $bs < 50\%$ for the red one.

further, the predicted stability optima were calculated for a maximum desirability set for $\Delta bs = 0$ and $\Delta h = 0$, aiming for no coalescence and no drainage (corresponding to the black dots).

Among the same applied limits, the three explored particles display different stability domains and optima. s-MC has a restricted stability domain, accessible only with an intense process. A high shearing rate is traditionally correlated to small droplets, which lead to a thicker texture and better stability. It can also be a clue for Pickering mechanisms because stability is only reached for high shearing energy intake (for particles to be irreversibly adsorbed at the oil−water interface). However, high particle concentration is needed which could indicate that, besides Pickering mechanisms, other phenomena can be considered: the more particles are incorporated in the system, the more they are likely to colonize the aqueous phase and form a 3D network entrapping the droplets and thereby contribute to stability [28]. Even if particle concentration can influence emulsion stability, the effect appears to be complex. The influence of the particle concentration on emulsion stability appears to be complex. While insufficient particle concentration results in incomplete interfacial coverage and instability, excessive concentration can lead to overcrowding and steric hindrance, similarly hindering emulsification. Therefore, a "viable" concentration range may exist for each particle type, balancing the stability without adverse effects. While the classification of such systems as "Pickering emulsions" is questionable due to the unknown predominant stabilization mechanism, the designation "particle-stabilized emulsion" remains highly appropriate.

On the other hand, semisoluble powders present larger stability territories. OP is quite versatile in terms of process intensity. Stable emulsions can be formulated using OP with an oil fraction from 40% up to 65% and a particle concentration between 2 and 12%. Regarding BC, its stability domain evolves depending on the applied process. For shorter emulsification time and low particle concentrations, BC powder allows reaching high oil concentrations (over 80%). Knowing that more than half of OP and BC total weight is soluble, this aqueous compatible fraction is likely to colonize the continuous phase as well as display an interfacial activity. This phenomenon may cause additional steric competition in an environment where the oil fraction and the excess particles are already filling up the available space and/or interface. It can also lead to synergistic mechanisms, resulting in improved stabilization.

These examples illustrate the importance of mastering the structuring mechanisms for formulating HIP(P)Es using solely

https://doi.org/10.1021/acsomega.4c08147
ACS Omega 2025, 10, 4534−4547

microparticles. A balance must be found among the oil fraction, the particle concentration, and the available aqueous fraction to contain it all. There must be enough particles to protect the interfaces and stabilize the emulsion, but not too many to avoid steric competition with the droplets. The CCD approach is a powerful tool to determine whether particles are compatible with HIPPE-like applications or not (and what are their equilibrium compositions).

Although soluble compounds can play a negative role in the total steric balance and/or act as competitors at the interfaces in some cases, they appear here to be of real interest, with OP and BC having large relative stability zones. Pickering effect, aqueous particle network, and soluble fraction are likely to interact positively. The impact of the soluble fraction may be of multiple types: (1) individual by thickening the continuous phase, trapping oil droplets in a gelled aqueous matrix[41] or reducing interfacial tension; (2) synergistic by helping particle interfacial colonization and structuration[24] or strengthening particle network. However, OP and BC do not share either the same soluble fraction or chemical composition. As OP is more expected to contain pectins and proteins,[40] the soluble fraction might act on both the interfacial region (amphiphilic proteins) and the continuous phase (pectins creating a gel-like network). Bentonite is an alkaline mineral (Al, Mg, Si, Na, Ca) mixture.[42] Even if it is known to form a particulate film around droplets,[43] the water-solubility of BC is not consensual and involves the very definition of solubility. According to the stance taken by this study, it corresponds to the elements that are still "solubilized" in water after strong centrifugation (no migration). Considering the $pH_{em.}$ of BC-based emulsions and the literature, these small elements must be charged and might interact with each other in the continuous phase, acting as a thickening agent. Considering these compositional differences, the studied particles are probably involved in different mechanisms.

Although OP and BC do not have the same sourcing and composition, these semisoluble particles appear to have more in common than OP and s-MC, even though the latter share a common cellulosic composition. Knowing that, combined mechanisms and complex particles seem to be key for the smart design of waterless systems. Moreover, OP and BC stability domains cover a wide range of formulations (including various textures as succinctly illustrated in Figure 5), from relatively fluid (E15) to firm or gelled matrices (E2). Among the stable samples formulated from the experimental design, the "texture gain" is directly correlated to the particle concentration increase. Their differences in the composition of the soluble species may explain the gap between the texture profiles of OP (more gelled) and BC (thicker), which supports the previous hypothesis about different stabilization mechanisms.

This preliminary study opens matrices opportunities by driving the formulation. The structure and its functionality can be tailored without compromising the relative stability. By defining stability maps, emulsion properties can be further explored whether by taking a closer look at the structuring role of the present species or by decorrelating the phenomena and their interactions through experimental designs. Many characterization measurements of emulsions require stable products to be carried out. As no missing data are allowed for experimental design, it is crucial to be able to guarantee a reliably stable working domain. This study aims to get around this problem using unusual indicators to overcome these constraints. After identifying a stable area and depending on the measurements realized, the experimental design approach could be used as a comprehensive and predictive tool to map emulsions' rheological, sensory, structural, and biological properties.

4. CONCLUSIONS

The present study offers a promising avenue for the development of sustainable cosmetic formulations by using stabilizing solid particles with minimal chemical modifications, adhering closely to "clean label" principles. The exploration of natural-based, relatively unmodified microparticles as building blocks for emulsion architectures delves into the potential of HIPPEs as a viable alternative to traditional water-filled and surfactant-based emulsions. This comparative analysis conducted on fourteen micrometric particles revealed significant variations in their ability to design waterless systems. Among all of the formulation parameters evaluated, the typology of particles appears as a prevalent factor over other elements (lipid phase, process, etc.). This highlights the importance of considering diverse sources, shapes, and chemical compositions when designing HIPPEs. Conventional particle parameters appear ineffective as selection criteria within this highly variable framework of natural-based systems, as demonstrated in previous examples. This suggests that established indicators of success do not readily translate to such highly concentrated and crowded environments. However, the particle soluble fraction emerges to be a key element in favor of their structuration, stabilization, and versatility. Selecting the appropriate microparticulate system is crucial for achieving the desired textural properties and stability. However, not all particles are equally sensitive to these parameters; some of them are more robust to formulation adjustments (like OP). Emulsion properties could be tailored by adjusting other compositional parameters, including the oil type or the process. Furthermore, through a targeted experimental design approach focusing on high-potential candidates, this study proposes the stabilization mechanisms at play within the studied architectures. By building a predictive model, this approach also suggests an actionable framework for industrial applications.

AUTHOR INFORMATION

Corresponding Author

Marie Cafiero − *AgroParisTech, UMR SayFood, Paris-Saclay University, Palaiseau 91123, France; INRAE, Palaiseau 91120, France; LVMH Recherche, Saint Jean de Braye 45800, France;* orcid.org/0000-0001-6557-4265; Email: marie.cafiero@agroparistech.fr

Authors

Marie-Noëlle Maillard − *AgroParisTech, UMR SayFood, Paris-Saclay University, Palaiseau 91123, France; INRAE, Palaiseau 91120, France*

Sabrina Maniguet − *LVMH Recherche, Saint Jean de Braye 45800, France*

Valérie de La Poterie − *LVMH Recherche, Saint Jean de Braye 45800, France*

Delphine Huc-Mathis − *AgroParisTech, UMR SayFood, Paris-Saclay University, Palaiseau 91123, France; INRAE, Palaiseau 91120, France*

Complete contact information is available at: https://pubs.acs.org/10.1021/acsomega.4c08147

https://doi.org/10.1021/acsomega.4c08147
ACS Omega 2025, 10, 4534−4547

Author Contributions

M.C. performed conceptualization, investigation, writing, and validation. M.-N.M. performed conceptualization and writing. S.M. performed conceptualization. V.dL.P. performed conceptualization. D.H.-M. performed conceptualization and writing.

Funding

This research was underwritten by LVMH Recherche, which contributed within the scope of Marie Cafiero's doctoral thesis (reference ANRT 2022/0064).

Notes

The authors declare no competing financial interest.

■ ACKNOWLEDGMENTS

The authors thank Léonie Gricourt for her help with the confocal laser scanning microscopy. Many thanks go to Jean-Marie Herry and Gilles Gerlot for the time spent to perform the contact angle measurements. This research was conducted as part of M. Cafiero's doctoral thesis, funded by ANRT and LVMH Recherche (contract number No. 2022/0064).

■ ABBREVIATIONS

O/W, oil-in-water; HIPE, high internal phase emulsion; HIPPE, high internal phase Pickering emulsion; NOI, natural origin index; CCD, central composite design; PCA, principal components analysis

■ REFERENCES

(1) Guyader, N. Contribution à la compréhension de l'évolution des propriétés multi-échelles des émulsions. (2022). Ph.D. Dissertation, CY Cergy Paris Université: France. 2022. https://theses.fr/2022CYUN1136/ (accessed 2024−06−20).

(2) Blue Gold *Water in Cosmetics*; Cosmetics Business, July 19, 2019. https://www.cosmeticsbusiness.com/news/article_page/Blue_gold_Water_in_cosmetics/156328 (accessed on 2024−06−20).

(3) Aguiar, J. B.; Martins, A. M.; Almeida, C.; Ribeiro, H. M.; Marto, J. Water sustainability: A waterless life cycle for cosmetic products. *Sustain. Prod. Consum.* **2022**, *32*, 35−51.

(4) Allan, J. A. Virtual Water - the Water, Food, and Trade NexusUseful Concept or Misleading Metaphor? *Water Int.* **2003**, *28* (1), 106−113.

(5) Martins, A. M.; Marto, J. M. A sustainable life cycle for cosmetics: From design and development to post-use phase. *Sustain. Chem. Pharm.* **2023**, *35*, No. 101178.

(6) Chung, C.; McClements, D. J. Structure−function relationships in food emulsions: Improving food quality and sensory perception. *Food Struct.* **2014**, *1*, 106−126.

(7) Lissant, K. J. The geometry of high-internal-phase-ratio emulsions. *J. Colloid Interface Sci.* **1966**, *22*, 462−468.

(8) Saiki, Y.; Prestidge, C. A.; Horn, R. G. Effects of droplet deformability on emulsion rheology. *Colloids Surf. A: Physicochem. Eng. Asp.* **2007**, *299*, 65−72.

(9) Rodriguez, A. M. B.; Binks, B. P. High internal phase pickering emulsions. *Curr. Opin. Colloid Interface Sci.* **2021**, *57*, No. 101556.

(10) Rebello, S.; Asok, A. K.; Mundayoor, S.; Jisha, M. S. Surfactants: Chemistry, Toxicity and Remediation. *Environ. Chem. a Sustain. World.* **2013**, *4*, 277−320.

(11) Berton-Carabin, C.; Schroën, K. Towards new food emulsions: designing the interface and beyond. *Curr. Opin. Food Sci.* **2019**, *27*, 74−81.

(12) Martini, M.-C. *Introduction à la cosmétologie*; Cosmetic Valley Editions: 2021, *177*, 978−2-490639−31−1.

(13) Bilal, M.; Iqbal, H. M. N. An insight into toxicity and human-health-related adverse consequences of cosmeceuticals — A review. *Sci. Total Environ.* **2019**, *670*, 555−568.

(14) Bursztejn, A.-C.; Rancé, F.; Barbaud, A. Protéines alimentaires des cosmétiques. *Rev. Fr. Allergol.* **2013**, *53*, 152−155.

(15) Binks, B. P. Particles as surfactants—similarities and differences. *Curr. Opin. Colloid In.* **2002**, *7*, 21−41.

(16) He, X.; Lu, Q. A review of high internal phase Pickering emulsions: Stabilization, rheology, and 3D printing application. *Adv. Colloid Interface Sci.* **2024**, *324*, No. 103086.

(17) Colver, P. J.; Bon, S. A. F. Cellular Polymer Monoliths Made via Pickering High Internal Phase Emulsions. *Chem. Mater.* **2007**, *19*, 1537−1539.

(18) Bolzinger, M. A.; Bordes, C.; Chevalier, Y.*Émulsions de Pickering en formulation cosmétique*; Techniques de l'ingénieur: 2024 .

(19) European Parliament *Commission Regulation (EU) 2018/1881 of 3 December 2018 amending Regulation (EC) No 1907/2006 of the European Parliament and of the Council on the Registration, Evaluation, Authorisation and Restriction of Chemicals (REACH) as regards Annexes I, III,VI, VII, VIII, IX, X, XI, and XII to address nanoforms of substances.* https://eur-lex.europa.eu/eli/reg/2018/1881/oj (accessed on 2024−06−20).

(20) Yang, T.; Zheng, J.; Zheng, B.; Liu, F.; Wang, S.; Tang, C. High internal phase emulsions stabilized by starch nanocrystals. *Food Hydrocoll.* **2018**, *82*, 230−238.

(21) Bai, Y.; Pei, X.; Zhao, B.; Xu, K.; Zhai, K.; Wang, C.; Zhang, F.; Tan, Y.; Zhang, B.; Wang, Y.; Wang, P. Multiple pickering high internal phase emulsions stabilized by modified diatomite particles via one-step emulsification process. *Chem. Eng. Sci.* **2020**, *212*, No. 115341.

(22) ISO16128−2:2017. *Cosmetics — Guidelines on Technical Definitions and Criteria for Natural and Organic Cosmetic Ingredients — Part 2: Criteria for Ingredients and Products*; International Organization for Standardization: 2017. https://www.iso.org/standard/65197.html (accessed on 2024−06−20).

(23) Huc-Mathis, D.; Cafiero, M.; Hollestelle, C.; Michon, C. One-step High Internal Phase Pickering Emulsions stabilized by uncracked micronized orange pomace. *Innov. Food Sci. Emerg.* **2022**, *79*, No. 103029.

(24) Hollestelle, C.; Michon, C.; Fayolle, N.; Huc-Mathis, D. Co-stabilization mechanisms of solid particles and soluble compounds in hybrid Pickering emulsions stabilized by unrefined apple pomace powder. *Food Hydrocoll.* **2024**, *146*, No. 109184.

(25) Zhang, L.; Zhou, C.; Xing, S.; Chen, Y.; Su, W.; Wang, H.; Tan, M. L. Sea bass protein-polyphenol complex stabilized high internal phase of algal oil Pickering emulsions to stabilize astaxanthin for 3D food printing. *Food Chem.* **2023**, *417*, No. 135824.

(26) Zielińska, A.; Wójcicki, K.; Klensporf-Pawlik, D.; Dias-Ferreira, J.; Lucarini, M.; Durazzo, A.; Lucariello, G.; Capasso, R.; Santini, A.; Souto, E. B.; Nowak, I. Chemical and Physical Properties of Meadowfoam Seed Oil and Extra Virgin Olive Oil: Focus on Vibrational Spectroscopy. *J. Spectrosc.* **2020**, *2020*, No. 8870170.

(27) Ferreira, M. S.; Magalhães, M. C.; Oliveira, R.; Sousa-Lobo, J. M.; Almeida, I. F. Trends in the Use of Botanicals in Anti-Aging Cosmetics. *Molecules.* **2021**, *26*, 3584.

(28) Lv, J.; Wang, H.; Zhu, M.; Chen, Q.; Huan, S.; Liu, Y.; Liu, S.; Li, Z.; Bai, Z. High internal phase Pickering emulsions via complexation of cellulose nanofibrils and nanochitin: Enhanced interfacial adsorption and structured aqueous network. *Food Hydrocolloids.* **2024**, *157*, No. 110383.

(29) Arditty, S. Fabrication, stabilité et propriétés rhéologiques des émulsions stabilisées par des particules colloïdales. (2007). Ph.D. Dissertation, Université Sciences et Technologies - Bordeaux I: France. 2007. https://theses.hal.science/tel-00135898/file/These_Stephane_Arditty.pdf (accessed 2024−06−20).

(30) Berton-Carabin, C. C.; Schroën, K. Pickering Emulsions for Food Applications: Background, Trends, and Challenges. *Annu. Rev. Food Sci. Technol.* **2015**, *6*, 263−297.

(31) McClements, D. J. Advances in fabrication of emulsions with enhanced functionality using structural design principles. *Curr. Opin. Colloid In.* **2012**, *17*, 235−245.

https://doi.org/10.1021/acsomega.4c08147
ACS Omega 2025, 10, 4534−4547

(32) Zlotogorski, A. Distribution of skin surface pH on the forehead and cheek of adults. *Arch. Dermatol. Res.* **1987**, *279*, 398−401.
(33) Murray, B. S. Pickering emulsions for food and drinks. *Curr. Opin. Food Sci.* **2019**, *27*, 57−63.
(34) Dickinson, E. Advances in food emulsions and foams: reflections on research in the neo-Pickering era. *Curr. Opin. Food Sci.* **2020**, *33*, 52−60.
(35) Joseph, C.; Savoire, R.; Harscoat-Schiavo, C.; Pintori, D.; Monteil, J.; Faure, C.; Leal-Calderon, F. Pickering emulsions stabilized by various plant materials: Cocoa, rapeseed press cake and lupin hulls. *LWT*. **2020**, *130*, No. 109621.
(36) Leal-Calderon, F.; Schmitt, V. Solid-stabilized emulsions. *Curr. Opin. Colloid Interface Sci.* **2008**, *13*, 217−227.
(37) de Folter, J. W. J.; Hutter, E. M.; Castillo, S. I. R.; Klop, K. E.; Philipse, A. P.; Kegel, W. K. Particle Shape Anisotropy in Pickering Emulsions: Cubes and Peanuts. *Langmuir* **2014**, *30* (4), 955−964.
(38) San-Miguel, A.; Behrens, S. Influence of Nanoscale Particle Roughness on the Stability of Pickering Emulsions. *Langmuir.* **2012**, *28* (33), 12038−12043.
(39) Schmitt, V.; Destribats, M.; Backov, R. Colloidal particles as liquid dispersion stabilizer: Pickering emulsions and materials thereof. *Comptes Rendus Physique.* **2014**, *15* (8−9), 761−774.
(40) Huc-Mathis, D.; Almeida, G.; Michon, C. Pickering emulsions based on food byproducts: A comprehensive study of soluble and insoluble contents. *J. Colloid Interface Sci.* **2021**, *581*, 226−237.
(41) Patel, A. R.; Dewettinck, K. Edible oil structuring: an overview and recent updates. *Food Funct.* **2016**, *7*, 20−29.
(42) de Carvalho-Guimarães, F. B.; Correa, K. L.; de Souza, T. P.; Rodríguez Amado, J. R.; Ribeiro-Costa, R. M.; Silva-Júnior, J. O. C. A Review of Pickering Emulsions: Perspectives and Applications. *Pharmaceuticals* **2022**, *15*, 1413.
(43) Khan, B. A.; Akhtar, N.; Khan, H. M. S.; Waseem, K.; Mahmood, T.; Rasul, A.; Iqbal, M.; Khan, H. Basics of pharmaceutical emulsions: A review. *Afr. J. Pharm. Pharmacol.* **2011**, *5*, 2715.

https://doi.org/10.1021/acsomega.4c08147
ACS Omega 2025, 10, 4534−4547